Appendices

A Comparison: Measured TFP and Identified *GDP* Shocks (Online appendix)

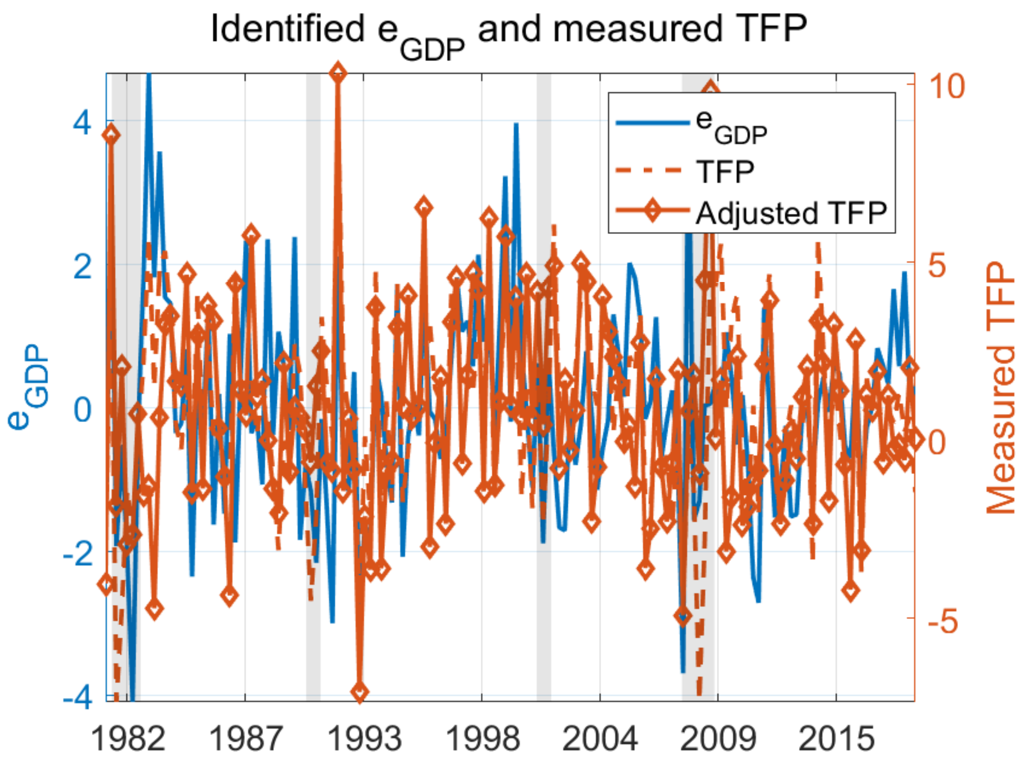

Figure 7: Comparison between identified GDP shocks and TFP. The blue solid line represents the identified GDP shocks e_{GDP} of the max-C solution. The red dashed line represents the growth rate of total factor productivity (TFP), and the red diamond line represents the growth rate of utilization-adjusted TFP using estimates from Basu et al. (2006). The shaded bars represent the NBER recession periods. The TFP data is downloadable at https://www.frbsf.org/economic-research/indicators-data/total-factor-productivity-tfp/. The correlation between TFP and e_{GDP} is 0.5838, and that between the adjusted TFP using estimates from Basu et al. (2006) and e_{GDP} is 0.3229. The data is quarterly from 1981 Q2 to 2018 Q3.

B Potential structural shocks: Set of all potential structural shocks (Online appendix)

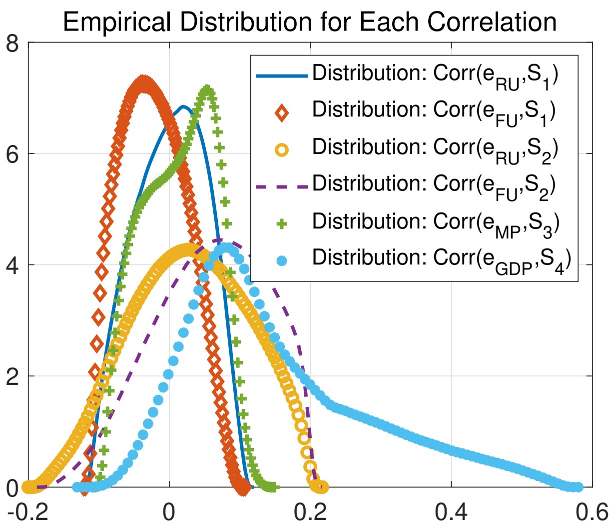

(a) Sample Distribution: Corr (Structural Shock, External Variable)

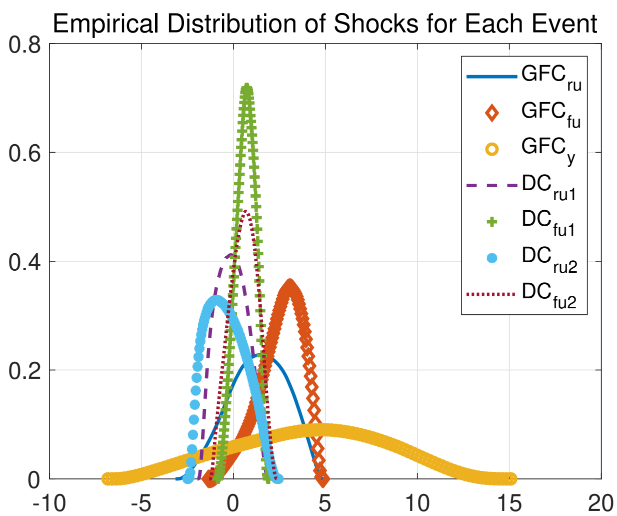

(b) Sample Distribution: Size of Structural Shock for Each Event

Figure 8: Sample Distribution from Simulation. Figure 8a depicts the kernel densities of correlations between structural shocks and external variables from all simulations. The blue solid line is the kernel density of correlation between the real uncertainty structural shocks (RU shocks, hereafter) and the stock returns. The red diamond depicts the correlation between the financial uncertainty structural shocks (FU shocks, hereafter). The yellow circle is the correlation between the RU shock and gold prices. The purple dotted line is the correlation between the FU shock and the gold price. The green cross is the correlation between the monetary policy shock and the Nakamura and Steinsson (2018) news shock, and the blue circle is the correlation between the real GDP structural shock and the measured TFP shock. Figure 8b depicts the kernel densities of the size of the structural shocks for each event. The blue solid line shows the kernel density for the size of the RU shocks at the month of the Lehman collapse. The red diamond shows the FU shocks in the month of the Lehman collapse. The yellow circle shows the real GDP shock during the GFC. The purple cross line shows the PCE shocks during the debt ceiling period in July 2011. The green dotted line shows the RU shocks during the debt ceiling period in July 2011. The sky blue cross shows the FU shock during the debt ceiling period in July 2011. The purple circle shows the RU shock during the debt ceiling period in August 2011. The sky blue colon shows the RU shocks during the debt ceiling period of August 2011, and the triangle shows the FU shock on Black Monday.

C Distributions of Identified Shocks (Online appendix)

In this section, we provide evidence that the max-C solution is indeed capable of serving as the representative solution of all the identified solutions. Figure 9 summarizes the evolution of the time series of the identified real and financial shocks. The shocks identified from the max-C solution are shown as the dotted line and the shaded band contains 99% of the set identified solutions. This figure clearly shows that all the identified series move in a quite similar manner compared to the max-C solution.

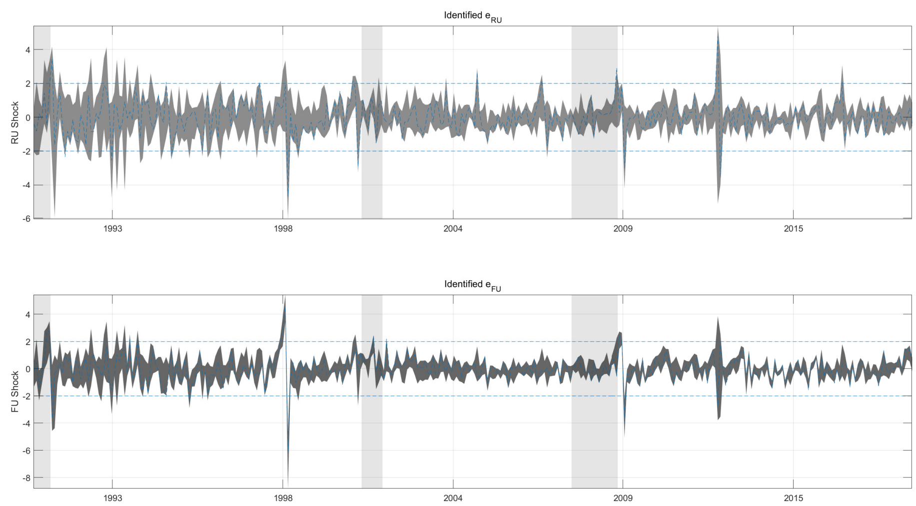

Figure 9: Time series of structural shocks of real and financial with the 99% bands. The shaded area and the thin lines represent the 90% and 68% confidence bands, respectively, and the solid lines represent the max-C impulse responses. and the shaded bands around the dotted lines are the 99% bands.

D Decomposing Endogenous Channels of Real and Financial Uncertainty (Online appendix)

We shut down the endogenous channels of real and financial uncertainty one at a time to isolate the influence of allowing endogeneity for each type of uncertainty. Figure 10a is the impulse response functions of the SVAR model when we do not allow endogenous financial uncertainty but do allow endogenous real uncertainty, and Figure 10b represents the opposite case. Our interest is in how real and financial uncertainty responds to the contractionary monetary policy shocks in each case. First, as shown in Figure 10a, while the response of real uncertainty is qualitatively the same as in the benchmark model, that of financial uncertainty is opposite once we shut down the endogenous feedback channel of financial uncertainty. Similarly, Figure 10b shows that while the response of financial uncertainty is the same with the benchmark model, that of real uncertainty becomes the opposite once we shut down the endogenous feedback channel of real uncertainty.

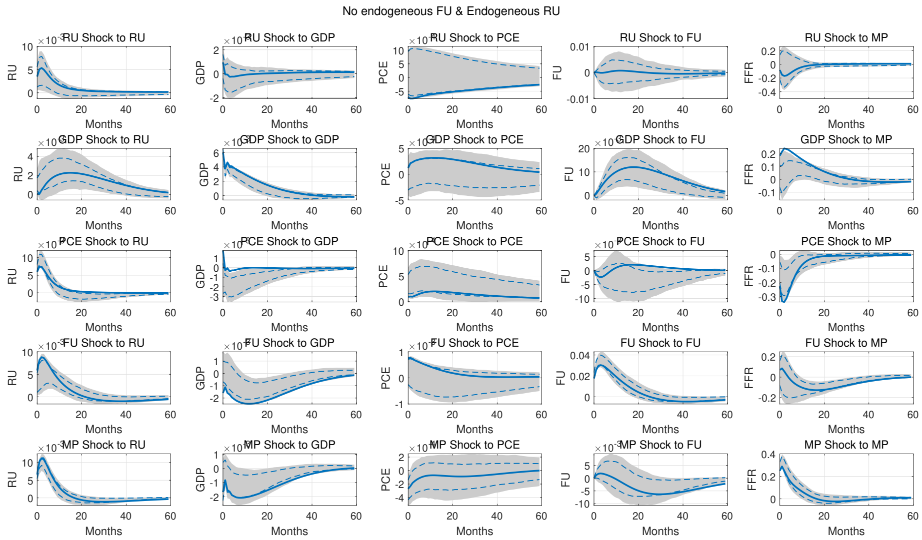

(a) Impulse response functions of the SVAR model when financial uncertainty does not respond endogenously but real uncertainty does. The shaded area and the dashed lines represent the 90% and 68% confidence bands, respectively, and the solid lines represent the max-C impulse responses.

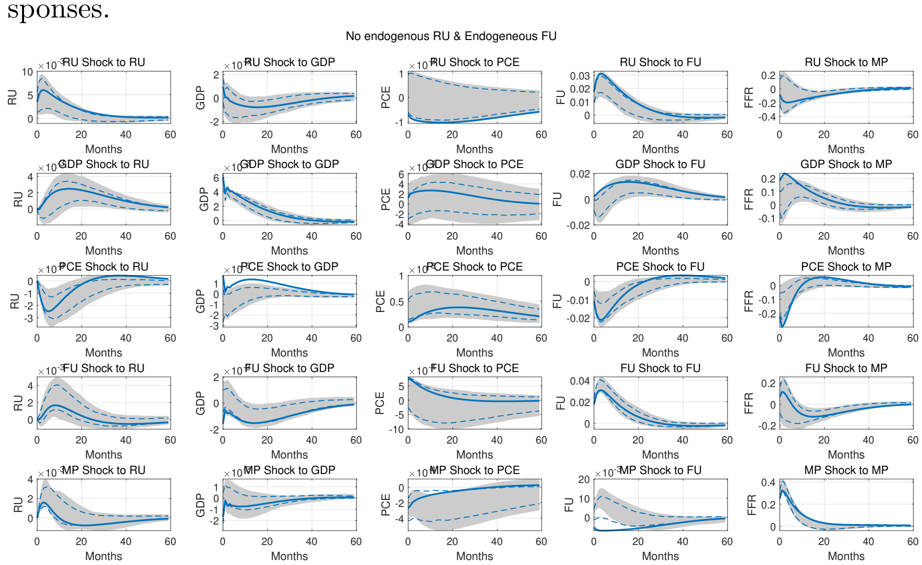

(b) Impulse response functions of the SVAR model when real uncertainty does not respond endogenously but financial uncertainty does. The shaded area and the dashed lines represent the 90% and 68% confidence bands, respectively, and the solid lines represent the max-C impulse responses.

Figure 10: Figure 10a represents the case of exogenous financial uncertainty, and Figure 10b represents the case of exogenous real uncertainty.

E Constructing the Confidence Intervals (Online appendix)

We construct the confidence intervals based on LMN. In particular, we use a bootstrap/Monte Carlo method to build the confidence intervals. Let R be the number of replications in a repeated sampling procedure. Let "hats" denote estimates from historical data, e.g., $\hat{e}_t$ represents estimated structural shocks. To denote simulated data, we use a "*". Accordingly, a "hat" is combined with a "*" to denote estimates from simulated data. To generate replicated samples of the structural shocks from the solution in a way that guarantees the events that happen in historical data also occur in the samples, we randomly draw with replacement from the estimates of the shocks, $\hat{e}_t$, with the exception that we fix the values for these shocks in each replication in the periods correspond to the event constraints. Since we identify a set of estimated parameters and shocks, we generate R samples of data from each estimated shocks in the set. Then, this is repeated for every solution in the identified set to obtain the confidence interval for the identified set of impulse responses.

Let M be the number of solutions in the identified set and m index an arbitrary solution in the set. Index each draw from the estimated structural shocks with r and denote the rth draw from the mth solution as e_t^{mr}. Each e_t^{mr} is combined with the B parameters of the mth solution, $\hat{B}^m$ to generate R samples of $\eta_t^{mr*} = \hat{B}^m e_t^{mr}$. Next, R new samples of X_T are generated recursively for each replication $r = 1, 2, \cdots, R$ using $X_t = \sum_{j=1}^{p} \hat{A}_j X_{t-j} + \eta_t^{mr*}$, with initial conditions fixed at their sample values. Using each of new samples, we fit a VAR(p) model to estimate new least squares estimates such as $\hat{\eta}_t^{mr*}, \hat{A}_1^{mr*}, \cdots, \hat{A}_p^{mr*}$.

To generate replicated samples of the external variables S_{1t} and S_{2t} from mth solution in a way that ensures the correlations with the estimated structural uncertainty shocks that appear in our historical data also occur in the simulated samples, we generate historical idiosyncratic stock market shocks e_{S1t}^{m} and gold price shocks e_{S2t}^{m} as the fitted residuals from regressions of S_{1t} and S_{2t} on a autoregressive lag and on $\hat{e}_t$. Next, we randomly draw with replacement from e^m_{S1t} and e^m_{S2t} with the exception that, as above, we fix the values for these shocks in each replication in the periods subject to the event constraints to obtain R new values e^{mr}_{S1t} and e^{mr}_{S2t} and R new values of S_{1t} and S_{2t} by recursively iterating on

$$S^{mr}_{1t} = d^m_{01} + \hat{\rho}_1 S^{mr}_{1t-1} + d^{m'}_1 e^{mr}_t + e^{mr}_{S1t} \tag{9}$$

$$S^{mr}_{2t} = d^m_{02} + \hat{\rho}_2 S^{mr}_{2t-1} + d^{m'}_2 e^{mr}_t + e^{mr}_{S2t} \tag{10}$$

with initial conditions fixed at their initial values. The parameters $\hat{\rho}_1$ and $\hat{\rho}_2$ are the sample estimates from a first-order autoregression of each variable in historical data. The parameters $d^{m'}_1$ and $d^{m'}_2$ are calibrated to match the observed correlations between the instruments and the estimated structural shocks for the mth solution in historical data so that $corr(S^{mr}_{1t}, e^{mr}_t)$ and $corr(S^{mr}_{2t}, e^{mr}_t)$ equal the observed historical correlations on average across all replications R.

We construct confidence intervals for the impulse response functions in repeated samples as follows. The number of replications is set to $R = 1,000$. Let $\Theta^{m,r,k}_{i,j,s}$ be the s-period ahead response of the ith variable to the shock j at the kth rotation, for replication r and solution m. Let $\underline{\Theta}^{m,r}_{i,j,s} = \min_k \Theta^{m,r,k}_{i,j,s}$ and $\overline{\Theta}^{m,r}_{i,j,s} = \max_k \Theta^{m,r,k}_{i,j,s}$. Each $(\underline{\Theta}^{m,r}_{i,j,s}, \overline{\Theta}^{m,r}_{i,j,s})$ pair presents the highest and lowest responses in replication r of solution m. From the quantiles of the set $\{\underline{\Theta}^{m,r}_{i,j,s}\}^{M,R}_{m=1,r=1}$ that includes all replications for all solutions we can obtain the $\alpha/2$ critical point. Similarly, from the quantiles of $\{\overline{\Theta}^{m,r}_{i,j,s}\}^{M,R}_{m=1,r=1}$, we have the $1 - \alpha/2$ critical point.

F Alternative threshold parameter: Case for $\bar{k}_{MP}$ is set to 75th percentile & $\bar{k}_y$ is set to 25th percentile (Online appendix)

In the benchmark criteria for choosing threshold parameter $\bar{k}$, we impose stronger criteria for $\bar{k}_M P$ and $\bar{k}_y$. In this section, we show that the stronger criteria does not change our main result. Figure 11 represents impulse responses functions for the case $\bar{k}_M P$ is set to 75th percentile and $\bar{k}_y$ is set to 25th percentile. Figure 11 shows that the main results are not changed by the alternative criteria even though we could have wider confidence intervals.

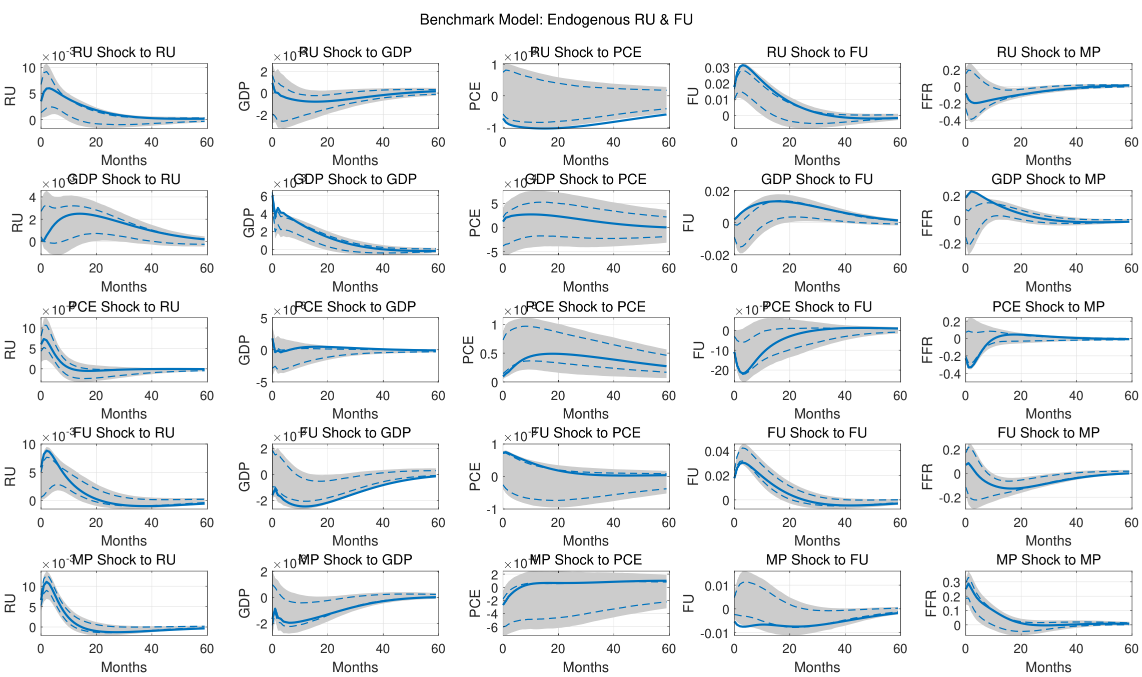

Figure 11: Impulse response functions when $\bar{k}_{MP}$ is set to 75th percentile & $\bar{k}_y$. The shaded area and the dashed lines represent the 90% and 68% confidence bands, respectively, and the solid lines represent the max-C impulse responses.